UNIVERSIDADE ESTADUAL PAULISTA
"JÚLIO DE MESQUITA FILHO"
FACULDADE DE CIÊNCIAS – BAURU
DEPARTAMENTO DE FÍSICA E METEOROLOGIA

Departamento de Física e Meteorologia
Bacharelado em Física de Materiais

Samuel Phelippe Bonetti

Caracterização superficial de ligas de alta entropia tratadas por oxidação por micro arco para potencial uso como biomateriais

Samuel Phelippe Bonetti

Orientador: Diego Rafael Nespeque Corrêa

Coorientadora: Jhuliene Elen Muro Torrento

Bauru
2025

Samuel Phelipe Bonetti

Caracterização superficial de ligas de alta entropia tratadas por oxidação por micro arco para potencial uso como biomateriais

Trabalho de Conclusão de Curso apresentado à Faculdade de Ciências – Câmpus de Bauru, da Universidade Estadual Paulista "Júlio de Mesquita Filho", para obtenção do grau de Bacharel em Física de Materiais.

Orientador: Diego Rafael Nespeque Correa

Coorientadora: Jhuliene Elen Muro Torrento

B712c

Bonetti, Samuel

Caracterização superficial de ligas de alta entropia tratadas por oxidação por micro arco para potencial uso como biomateriais / Samuel Bonetti. -- Bauru, 2025

40 p.

Trabalho de conclusão de curso (Bacharelado - Física) - Universidade Estadual Paulista (UNESP), Faculdade de Ciências, Bauru

Orientador: Diego Rafael Nespeque Corrêa

Coorientadora: Jhuliene Elen Muro Torrento

1. biomateriais metálicos. 2. ligas de alta entropia. 3. oxidação por micro arco. 4. cobre. 5. biofuncionalização. I. Título.

Sistema de geração automática de fichas catalográficas da Unesp. Dados fornecidos pelo autor(a).

Samuel Phelipe Bonetti

Caracterização superficial de ligas de alta entropia tratadas por oxidação por micro arco para potencial uso como biomateriais

Trabalho de Conclusão de Curso apresentado à Faculdade de Ciências – Câmpus de Bauru, da Universidade Estadual Paulista "Júlio de Mesquita Filho", para obtenção do grau de Bacharel em Física de Materiais.

Banca examinadora:

Prof. Dr. Diego Rafael Nespeque Correa

Dra. Mariana Luna Lourenço

Me. Israel Ramos Rodrigues

Aprovado em: 9 de dezembro de 2025

ATA DE DEFESA PÚBLICA DO TRABALHO DE CONCLUSÃO DE CURSO

Aos 09 dias do mês de dezembro de 2025, às 14h00, em sessão pública em formato presencial\virtual via Google Meet, na presença da Banca Examinadora presidida pelo **Prof. Dr. Diego Rafael Nespeque Correa** e composta pelos examinadores **Dra. Mariana Luna Lourenço** e **Me. Israel Ramos Rodrigues**, o aluno **Samuel Phelippe Bonetti** apresentou o trabalho de conclusão de curso intitulado: **"Caracterização superficial de ligas de alta entropia tratadas por oxidação por micro arco para potencial uso como biomateriais",** como requisito curricular indispensável para a integralização do curso de Física – Bacharelado em Física de Materiais. Após reunião em sessão reservada, a Banca Examinadora deliberou e decidiu pela **aprovação** do referido trabalho, divulgando o resultado formalmente ao aluno e demais presentes e eu, na qualidade de Presidente da Banca, lavrei a presente ata que será assinada por mim, pelos demais examinadores e pelo aluno.

gov.br Documento assinado digitalmente
DIEGO RAFAEL NESPEQUE CORREA
Data: 09/12/2025 15:56:35-0300
Verifique em https://validar.iti.gov.br

_____
Orientador

gov.br Documento assinado digitalmente
MARIANA LUNA LOURENCO
Data: 11/12/2025 06:57:48-0300
Verifique em https://validar.iti.gov.br

_____
Membro 1

gov.br Documento assinado digitalmente
ISRAEL RAMOS RODRIGUES
Data: 11/12/2025 07:22:10-0300
Verifique em https://validar.iti.gov.br

_____
Membro 2

gov.br Documento assinado digitalmente
SAMUEL PHELIPPE BONETTI
Data: 11/12/2025 07:28:44-0300
Verifique em https://validar.iti.gov.br

_____
Aluno

Dedico este trabalho aos meus pais e minha família, os quais sempre apoiaram minhas decisões e incentivaram meus estudos.

AGRADECIMENTOS

Agradeço ao meu orientador, Prof. Dr. Diego Rafael Nespeque Corrêa, pela confiança depositada ao longo de todo este período, pelas orientações, incentivos e pela constante dedicação. Sua paixão pela Física é verdadeiramente inspiradora e contagiante, tornando os desafios da pesquisa mais leves e, muitas vezes, agradáveis. Foi mais que um orientador e sim um amigo durante todo esse período.

Aos meus colegas de curso, expresso minha sincera gratidão pela convivência e pela colaboração, tanto nos estudos quanto nos momentos de descontração, que foram essenciais para renovar as energias nos períodos mais exigentes dessa jornada. Espero que isso seja apenas o começo e possamos continuar todos juntos.

Aos membros do laboratório, agradeço por todo o aprendizado e auxílio prestados em cada etapa do trabalho. Em especial, ao professor Beto, por seu acolhimento, ensinamentos e conselhos, seja durante os congressos, nas reuniões do grupo ou nos momentos de descontração. Seu exemplo e incentivo foram fundamentais.

Agradeço, ainda, a todos os professores que contribuíram para minha formação, seja em sala de aula ou em outras atividades acadêmicas. Cada um, à sua maneira, colaborou para o meu desenvolvimento não apenas intelectual, mas também pessoal, transmitindo valores e princípios que levarei comigo ao longo da vida.

Meus agradecimentos aos meus país que estiveram junto comigo durante todo esse tempo me incentivando e fortalecendo, nada disso seria possível sem eles.

Meus agradecimentos ao CNPQ (100704/2024-7) e Fapesp (2025/02091-0 e 2024/14878-2) por todo apoio financeiro e infraestrutural, além de diversos incentivos que contribuíram muito para minha formação.

“não tenho certeza de nada, mas a visão das estrelas me faz sonhar”

- Vincent Van Gogh

Caracterização superficial de ligas de alta entropia tratadas por oxidação por micro arco para potencial uso como biomateriais

RESUMO

Este estudo visou funcionalizar a superfície de uma liga de alta entropia TiZrNbTaMo, utilizando a técnica de oxidação por micro arco (MAO) com eletrólito rico em íons de cálcio, fosforo, magnésio e cobre buscando também uma ação antimicrobiana. Foi investigado o impacto da variação da concentração de cobre na morfologia, composição de fases, estrutura química, molhabilidade e citocompatibilidade dos revestimentos formados. Os resultados mostraram que a amostra sem modificação de superfície continha predomínio de fase (CCC) e fases minoritárias de (HCP), já as amostras tratadas exibiram predomínio de fase (CCC) com uma região amorfa com picos de $CaCO_3$, CaO e $CaPO_4$. As análises por EDS, FTIR, Raman e XPS confirmaram a incorporação de elementos bioativos (Ca, P, Mg) e traços de Cu_2O. As análises de superfície mostraram que o tratamento de MAO aumentou a rugosidade das amostras e a adição do cobre no eletrólito aumentou a hidrofilicidade, favorecendo a adesão celular. As análises dos testes in vitro com células MC3T3-E1 demonstraram que a adição de cobre não provocou citotoxicidade, mas, ao contrário, favoreceu a viabilidade e a adesão celular. Portanto a utilização de MAO com eletrólito enriquecido em cobre se destaca como uma estratégia promissora para funcionalizar materiais voltados a aplicações ortopédicas em dispositivos de fixação óssea.

Palavras-chave: biomateriais metálicos; ligas de alta entropia; oxidação por micro arco; cobre; biofuncionalização.

Surface characterization of high-entropy alloys treated by micro-arc oxidation for potential use as biomaterials.

ABSTRACT

This study aimed to functionalize the surface of a high-entropy alloy TiZrNbTaMo using the micro-arc oxidation (MAO) technique with an electrolyte rich in calcium, phosphorus, magnesium, and copper ions, also seeking to provide antimicrobial activity. The impact of varying copper concentration on the morphology, phase composition, chemical structure, wettability, and cytocompatibility of the formed coatings was investigated.The results showed that the untreated sample contained a predominant (BCC) phase and minor (HCP) phases, whereas the treated samples exhibited a predominant (BCC) phase along with an amorphous region characterized by peaks of $CaCO_3$, CaO, and $CaPO_4$. Analyses by EDS, FTIR, Raman, and XPS confirmed the incorporation of bioactive elements (Ca, P, Mg) and traces of Cu_2O. Surface analyses revealed that the MAO treatment increased the sample roughness, and the addition of copper to the electrolyte enhanced hydrophilicity, promoting cell adhesion. In vitro tests using MC3T3-E1 cells demonstrated that copper addition did not induce cytotoxicity but, on the contrary, improved cell viability and adhesion. Therefore, the use of MAO with a copper-enriched electrolyte stands out as a promising strategy to functionalize materials intended for orthopedic applications in bone fixation devices.

Keywords*: metallic biomaterials; high entropy alloys; micro-arc oxidation; copper; biofunctionalization.*

SUMÁRIO

1 Introdução

1.1 Biomateriais metálicos

Apesar do uso disseminado de metais e ligas na área biomédica, ainda há necessidade de desenvolver novos materiais para aplicação no corpo humano, a fim de atender às demandas clínicas atuais e aos avanços no tratamento de traumas, lesões e doenças. Assim, a otimização das propriedades dos biomateriais metálicos pode resultar em melhor biocompatibilidade e redução das rejeições decorrentes de complicações pós-cirúrgicas de implantes, além de proporcionar maior durabilidade e resistência para uso a longo prazo e atenuar o efeito de blindagem nos ossos (Abdel-Hady Gepreel; Niinomi, 2013; Davis et al., 2022; Thanigaivel et al., 2022). Portanto, é fundamental para a medicina moderna desenvolver novos biomateriais com propriedades favoráveis ao uso prolongado no corpo humano.

Ao mesmo tempo, a demanda por implantes metálicos, especialmente nas áreas de ortopedia e odontologia, tem crescido consideravelmente ao longo dos anos em todo o mundo devido a diversos fatores. O crescimento populacional, aliado ao envelhecimento da população, tem favorecido o surgimento de problemas relacionados à idade, como artrite e osteoporose, que exigem dispositivos para substituir e reparar ossos e articulações (J Bijlsma et al., 2011; Karaflou; Goulis, 2025; Maradit Kremers et al., 2015). A ocorrência de traumas e lesões causados por acidentes de trânsito, práticas esportivas e conflitos armados é outro fator a ser considerado, visto que esses eventos resultam em danos significativos à estrutura óssea do corpo humano.

Por fim, o aumento global do poder aquisitivo e os avanços nos tratamentos médicos voltados a traumas e lesões tornaram o uso de implantes mais acessível à população, contribuindo também para o crescimento desse mercado (Mahmud et al., 2023; Tharani Kumar et al., 2020). Desse modo, a pesquisa e o desenvolvimento de novos biomateriais metálicos são essenciais e podem resultar em avanços significativos na qualidade de vida e no bem-estar da população.

1.2 Ligas de alta entropia

As ligas de alta entropia (*High Entropy Alloys* - HEAs) surgiram nos primeiros anos do século XXI e, atualmente, são reconhecidas por suas propriedades singulares (Gao et al., 2022). Ao combinar cinco ou mais elementos de liga em proporções quase equiatômicas em uma solução sólida é possível obter alta entropia configuracional, grande distorção da rede cristalina, difusão atômica reduzida e o chamado efeito coquetel, fatores que contribuem para o aprimoramento de suas propriedades em diversas aplicações industriais, como nos setores de

infraestrutura, naval, aeronáutico, energético, catalítico e biomédico (Miracle; Senkov, 2017; Yu et al., 2024). Essa configuração elementar complexa é responsável pelas características de desempenho únicas apresentadas pelas HEAs.

Do ponto de vista termodinâmico, a entropia (ΔS) quantifica o grau de desordem em um sistema. O aumento da entropia de mistura suprime, de forma eficaz, a formação de compostos intermetálicos complexos e favorece o desenvolvimento de soluções sólidas homogêneas de fase única, como estruturas cúbicas de faces centradas (CFC), cúbicas de corpo centrado (CCC) ou hexagonais compactas (HC) (Xu et al., 2019). No entanto, quando a disparidade entre os tamanhos atômicos é excessiva, pode ocorrer uma distorção significativa da rede cristalina, potencialmente levando à formação de estruturas amorfas. Notavelmente, essas distorções na rede cristalina não apenas aumentam a dureza e a resistência do material, mas também melhoram sua estabilidade sob condições de alta temperatura e pressão (Kim et al., 2018).

Além disso, o chamado efeito de difusão lenta, decorrente das grandes diferenças nas taxas de difusão atômica entre os elementos constituintes, reduz a mobilidade atômica em temperaturas elevadas, retardando, assim, as transformações de fase e o crescimento de grãos (Ng et al., 2012).

Por fim, o efeito coquetel, que combina sinergicamente as propriedades intrínsecas dos diferentes elementos, contribui para aprimorar ainda mais o desempenho mecânico, bem como a resistência à corrosão e à oxidação das HEAs (Hsu et al., 2024a).

Coletivamente, esses efeitos conferem às ligas de alta entropia um desempenho superior em comparação às ligas metálicas convencionais. Como resultado, dada a ampla variedade de soluções sólidas possíveis, as HEAs consolidaram-se recentemente como um campo promissor a ser explorado.

Na área biomédica, as HEAs têm se destacado nos últimos anos como uma nova alternativa para a fabricação de implantes ortopédicos e dentários, em substituição a materiais tradicionais, como o titânio e suas ligas, o aço inoxidável e as ligas de cobalto-cromo. Essa substituição deve-se principalmente às suas propriedades vantajosas, como elevada resistência à corrosão e ao desgaste em diferentes ambientes químicos, além de um equilíbrio adequado entre resistência mecânica e ductilidade. (Lv et al., 2025)

As ligas de alta entropia atualmente desenvolvidas para uso como biomateriais são, em sua maioria, baseadas em titânio, uma vez que esse elemento já apresenta diversas propriedades otimizadas para aplicação no corpo humano, especialmente biocompatibilidade e capacidade de osseointegração como exemplificado pela HEA equiatômica TiZrNbMoTa, a qual foi foi uma

das primeiras ligas de alta entropia (HEAs) projetadas para uso como implantes ortopédicos (Bio-HEA), devido à sua composição química não tóxica e não alergênica. Os resultados anteriores indicaram uma fase cúbica de corpo centrado (BCC) na forma de grãos equiaxiais, o que garantiu alta resistência mecânica, baixo módulo de elasticidade, elevada resistência à corrosão e biocompatibilidade adequada.(Castro et al., 2021; Ma et al., 2020). Porém a literatura ainda carece de estudos acerca de funcionalização de superfície dessas ligas de alta entropia visando aplicações como biomateriais.

1.3 Oxidação por micro arco

A funcionalização da superfície de metais e ligas é crucial para a otimização de suas propriedades e do desempenho em uma ampla gama de aplicações tanto nas áreas de biomateriais quanto na própria indústria. Esse processo melhora significativamente a interação do material com o ambiente, resultando em benefícios como maior resistência à corrosão, melhor adesão de revestimentos protetores e efeito antimicrobiano (Rotella et al., 2024). Esses fatores são especialmente importantes em biomateriais, nos quais a durabilidade e a segurança dos materiais em contato com o corpo humano são de extrema relevância.

Entre as diversas técnicas de modificação de superfícies metálicas, a oxidação micro arco (*Micro-Arc Oxidation* - MAO) tem se destacado como uma das principais ferramentas aplicadas em implantes à base de titânio. A técnica baseia-se na aplicação de um potencial anódico à superfície do titânio imerso em um eletrólito, promovendo o crescimento de uma camada de óxido por meio da geração de descargas de plasma decorrentes da ruptura dielétrica. O processo resulta em um revestimento espesso, firmemente aderido ao substrato, poroso e enriquecido com espécies químicas provenientes do eletrólito (Ming et al., 2023a; Wen et al., 2023).

Com base nisso, diversos estudos têm destacado os efeitos benéficos do MAO em titânio e suas ligas para aplicação como biomateriais, especialmente na melhoria da biocompatibilidade, da resistência à corrosão e da bioatividade. No entanto, os estudos envolvendo o uso da MAO em HEAs ainda são escassos na literatura.

Zhang e colaboradores (Zhang et al., 2023) foram pioneiros na combinação da técnica MAO com HEAs para uso biomédico. Os autores submeteram a liga TiNbTaZrHf ao tratamento por MAO utilizando uma fonte de corrente alternada (CA) a 500 Hz, 40%, durante 5 minutos, com potencial anódico entre 150 e 250 V, em um eletrólito composto por NaOH, $Ca(CH_3COO)_2 \cdot H_2O$ e $Na_2SiO_3 \cdot 9H_2O$. Os resultados indicaram um grande potencial para aplicação como biomaterial, uma vez que o tratamento gerou uma camada de óxido porosa

predominantemente amorfa, contendo nanocristais de $Hf_{0,5}Zr_{0,5}O_2$ e enriquecida com íons bioativos. Essas características mostraram impacto positivo na resistência à corrosão e ao desgaste, bem como na citotoxicidade *in vitro* em contato com células osteoblásticas.

Nesse contexto, Sousa e colaboradores (Sousa et al., 2024a), realizaram um tratamento inovador por MAO em algumas HEAs desenvolvidas especificamente para uso como biomateriais, baseadas em TiZrNbTaMo, TiZrNbTaMn e TiZrNbFeMo. O processo utilizou um eletrólito rico em Ca, P e Mg, com variação de potencial anódico entre 100 e 300 V, empregando uma fonte de corrente contínua (CC). Os resultados foram promissores para aplicações em implantes, uma vez que as superfícies das ligas apresentaram características distintas quanto ao tamanho de poros, espessura, molhabilidade, absorção de íons bioativos, cristalinidade e oxidação dos elementos de liga, variando diretamente conforme a composição química e a microestrutura do substrato.

Sabe-se que os implantes são mais suscetíveis à colonização bacteriana nas primeiras 6 horas após a implantação (He et al., 2016). Portanto, os mecanismos de ação antibacteriana devem operar principalmente durante o período pós-operatório inicial, por isso metais com ação antibacteriana (como Ag, Cu, Pt e Sr) têm sido utilizados no eletrólito para funcionalizar os revestimentos, proporcionando atividade bactericida adequada contra diferentes linhagens bacterianas. Por exemplo, Cardoso e colaboradores (Cardoso et al., 2023a) empregaram a técnica de oxidação microarco (MAO) para incorporar cobre na liga Ti-30Nb-5Mo, destinada a aplicações biomédicas, e observaram que a incorporação de Cu nos revestimentos melhorou significativamente a atividade antimicrobiana da superfície, apresentando excelente desempenho contra *Escherichia coli* (E. coli) e *Staphylococcus aureus* (S. aureus).

A presença de cobre no eletrólito mostra-se, portanto, uma estratégia promissora para aprimorar a ação antibacteriana, podendo, quando utilizada adequadamente, promover de forma eficaz a proliferação de células osteoblásticas. No entanto, o excesso desses elementos pode levar à citotoxicidade dos materiais (He et al., 2016; Zhang et al., 2018). Assim, se mostram necessários mais estudos adicionais variando a concentração de cobre no eletrólito e avaliando sua influência sobre as propriedades do filme e sua biocompatibilidade.

Como um resultado, novos estudos sobre recobrimentos em superfícies de HEAs por MAO podem trazer resultados originais e inovadores para futuras aplicações como biomateriais, sem grande aumento no seu custo de processamento, o que torne viável a sua comercialização.

2 Objetivos

O presente projeto teve como objetivo desenvolver e caracterizar um novo material com potencial aplicação como biomaterial, por meio da funcionalização de uma HEA TiZrNbTaMo utilizando a técnica de revestimento superficial por MAO. O eletrólito empregado foi enriquecido com íons de cálcio, fósforo, magnésio e cobre, sendo este último variado em concentração, a fim de avaliar o impacto dessa variação nas propriedades químicas, físico-químicas, estruturais, topográficas e uma análise inicial de biocompatibilidade do material. Dessa forma, o estudo visou estabelecer correlações entre a modificação superficial promovida pelo MAO e o desempenho biológico do material, contribuindo para o desenvolvimento de revestimentos multifuncionais voltados a aplicações ortopédicas de fixação óssea.

3 Capítulo único

Este trabalho será apresentado no formato de artigo completo, sendo transcrito abaixo semelhante à forma que foi submetido no periódico científico *Materials* na seção *Metals and Alloys* edição especial *New Advances in High Entropy Alloys*

Surface engineering of non-equiatomic TiZrNbTaMo HEA by MAO treatment in a Cu-rich electrolyte for biomedical applications

Samuel Phelippe Bonetti[1], Jhuliene Elen Muro Torrento[1], Carlos Roberto Grandini[1], Tiago dos Santos Pereira de Sousa[2], Gerson Santos de Almeida[3], William Fernando Zambuzzi[3], Diego Rafael Nespeque Correa[1,*]

[1]São Paulo State University (UNESP), School of Sciences, Campus Bauru, Laboratory of Anelasticity and Biomaterials, 17.033-360 Bauru, SP, Brazil

[2]São Paulo State Technological College (FATEC), Bauru Campus, 17033-360 Bauru, SP, Brazil

[3]São Paulo State University (UNESP), Institute of Biosciences, Department of Chemistry and Biochemistry, 18618-689, Botucatu, SP, Brazil

*Corresponding author: diego.correa@unesp.br

ABSTRACT

This study evaluates the surface functionalization of a non-equiatomic TiZrNbTaMo high-entropy alloy (HEA) by micro-arc oxidation (MAO) in Cu-rich electrolytes to tailor its performance for biomedical implants. The Cu content was varied, and the resulting coatings were assessed for their morphology, phase constitution, chemical structure, wettability, and cytocompatibility. XRD of the substrate indicated a body-centered cubic (BCC) matrix with minor HCP features; after MAO, predominantly amorphous oxide layers formed with sparse reflections assignable to $CaCO_3$, CaO, and $CaPO_4$. FTIR/Raman/XPS identified stable oxides (TiO_2, ZrO_2, Nb_2O_5, Ta_2O_5,

MoO_3) and the incorporation of bioactive elements (Ca, P, Mg) together with trace Cu, mainly as Cu_2O; EDS corroborated these compositions. MAO increased surface roughness and rendered the surfaces hydrophilic, features typically favorable to osseointegration. In vitro assays with MC3T3-E1 cells (24 h) showed that Cu addition did not induce cytotoxicity, maintaining or improving cell viability and adhesion compared to controls. Collectively, MAO in Cu-rich media yields porous, bioactive, Cu-incorporated oxide coatings on TiZrNbTaMo HEA, preserving cytocompatibility and supporting their potential for orthopedic and bone-fixation applications.

Keywords: metallic biomaterials; high entropy alloys; micro-arc oxidation; copper; biofunctionalization.

1. INTRODUCTION

Bone is a dynamic, vascularized, and metabolically active tissue whose regeneration demands materials that restore function, structural integrity, and biological integration (Van der Eerden; Teti; Zambuzzi, 2014). On this matter, high-entropy alloys (HEAs) are a promising category of multicomponent alloys, typically composed of five or more elements in equiatomic or near-equiatomic proportions (5-35 at%), developed to overcome the limitations of existing alloys in certain engineering applications (Hsu et al., 2024b). Conventionally, the recently developed HEAs exhibit unique characteristics, such as superior mechanical strength, corrosion and wear resistance, and thermal stability compared to conventional metallic materials, because of the combination of configurational entropy, sluggish diffusion, lattice distortion, and cocktail effect (Li et al., 2025). Thus, the research and development of high-entropy materials has the potential to deliver significant advances in engineering applications.

Recently, HEAs have been considered for use as biomaterials, with a focus on load-bearing implants for hard-tissue replacements. Currently, HEAs are among the most promising alloys for medical devices, as certain compositions have proven to be biologically safe, highly corrosion- and wear-resistant in simulated body conditions, and capable of forming simple crystalline structures with high ductility (Adhikari et al., 2025). These characteristics align with the typical attributes of metallic biomaterials, indicating strong potential for biomedical applications. The equiatomic Ti-Zr-Nb-Ta-Mo HEA (TiZrNbTaMo) has been extensively studied for biomedical implant applications (Todai et al., 2017). For example, Hua *et al.* (Hua et al., 2021) conducted mechanical analyses and compared them with those of the biomedical Ti-6Al-4V alloy. Their

findings indicate that TiZrNbTaMo performed better in biological environments due to its superior combination of properties. Furthermore, Wang and Xu (Wang; Xu, 2017) performed mechanical and corrosion analyses on this composition and found that TiZrNbTaMo HEA demonstrated excellent corrosion resistance in PBS (Phosphate Buffered Saline solution), comparable to that of the Ti-6Al-4V alloy, and pitting resistance that was remarkably superior to that of the SS 316L and CoCrMo alloys. However, because its surface is bioinert, surface modification techniques are crucial for enhancing interaction with adjacent bone tissues when used in the human body.

Among the various surface modification techniques, micro-arc oxidation (MAO) has established itself as a powerful tool for titanium-based implants (Li et al., 2023). The technique is focused on applying an anodic potential to the surface of titanium immersed in an electrolyte, ensuring the growth of the oxide layer with the generation of plasma discharges by dielectric breakdown, resulting in a thick coating, firmly adhered to the substrate, porous, and enriched by chemical species from the electrolyte (Ming et al., 2023b). Thus, the formation of porous oxide coatings enriched with strategically selected chemical species can provide superior biocompatibility, osseointegration, and biofunctionality (Ming et al., 2023b). In Ti-based alloys, MAO treatment has been successfully applied to produce Ca- and P-rich coatings, which are recognized for their bioactivity in promoting rapid bone recovery and growth. Furthermore, antibacterial metals (e.g., Ag, Cu, Pt, and Sr) have been used in the electrolyte to decorate the coatings, providing adequate bactericidal activity against distinct bacterial lineages and mitigating biofilm formation (He et al., 2017). For example, Cardoso *et al.* (Cardoso et al., 2023b) used the MAO technique to incorporate copper into the Ti-30Nb-5Mo alloy for biomedical applications, finding that the incorporation of Cu into the coatings improved the antimicrobial activity of the surface and exhibited excellent antibacterial activity against *Escherichia coli* (*E. coli*) and *Staphylococcus aureus* (*S. aureus*).

Considering that the physicochemical aspects of Ti-based high entropy alloys are not the same as those of conventional Ti alloys, studies about the production of antibacterial coatings in HEAs by MAO treatment deserve to be explored. Accordingly, rigorous in vitro cytotoxicity evaluation is a prerequisite to any claim of antimicrobial benefit for Cu-containing MAO coatings. Complementary colorimetric assays should be employed: MTT quantifies mitochondrial dehydrogenase activity (metabolic viability), while crystal violet measures adherent cell biomass (attachment/proliferation) (Cardoso et al., 2022; Fernandes et al., 2023). Used in 24-72 h exposure and dose-response formats with appropriate controls, these orthogonal endpoints increase

sensitivity to sublethal mitochondrial dysfunction and anti-adhesive effects, reduce false negatives, and enable definition of biocompatible materials in accordance with ISO 10993-5/-12 principles and justify further progression to in vivo evaluation as we have widely discussed (Gemini-Piperni et al., 2014; Zambuzzi et al., 2011; Zambuzzi; Ferreira, 2025).

Here, we sought to functionalize the surface of a TiZrNbTaMo high-entropy alloy (HEA) by applying micro-arc oxidation (MAO) in a Cu-rich electrolyte to probe the influence of Cu on the resulting oxide coating and its suitability for biomedical implants. Following MAO, specimens were systematically characterized for surface topography, chemical composition, phase constitution, roughness, wettability, Vickers microhardness, and in vitro cytotoxicity, enabling a comprehensive assessment of Cu-mediated effects on coating properties and biocompatibility.

2. MATERIAL AND METHODS

2.1. Sample synthesis

An ingot (30 g) was produced from commercially pure metals (Ti, Zr, Nb, Ta, and Mo; purity > 99%) that had been previously separated into equiatomic proportions. The metals were ultrasonically cleaned in an acetone bath for 10 minutes (0.6 ks). Afterward, the metals were melted in an arc-melting furnace under an inert argon atmosphere, using a non-consumable tungsten electrode and a water-cooled copper crucible. The ingot was remelted 7 times to ensure complete mixing of the alloying elements. Then, the ingots underwent a homogenization heat treatment at 10^{-6} Torr, with a heating rate of approximately 10 $K \cdot min^{-1}$, a temperature plateau of 1273 K for 12 hours (43.2 ks), followed by slow cooling to room temperature.

2.2. Surface treatment

The ingot was sectioned into approximately 2 mm-thick lamellar samples using a cutting machine (ISOMET 100, USA). After that, the samples were cold mounted in acrylic resin and ground on waterproof SiC papers (until 1200 mesh). Before surface treatment, the samples were removed from the resin and cleaned in an ultrasonic acetone bath for 10 minutes, followed by another cleaning cycle in distilled water. The MAO treatment was conducted at 300 V, with a limited current of 2.5 A, for 0.6 ks. A digital multimeter (Keysight, model N5751A, USA) and a

computer were used to record the current through the sample during the process. The electrolyte was composed of distinct proportions of calcium acetate (CaA; $Ca(C_2H_3O_2)_2$), β-calcium glycerophosphate (β-GP; $C_3H_7CaO_6P$), magnesium acetate (MgA; $Mg(C_2H_3O_2)_2$), and copper acetate (CuA; $Cu(C_2H_3O_2)_2$), following earlier studies from the literature (Sousa et al., 2024b). The electrolyte was previously magnetically stirred for 1 hour (3.6 ks) to ensure a complete mixing of the reagents. The studied samples and their corresponding electrolyte compositions are presented in **Table 1**.

Table 1: Nomenclature of the samples and the corresponding composition of the electrolyte.

Sample	Electrolyte			
	CaA (mol·L^{-1})	β-GP (mol·L^{-1})	MgA (mol·L^{-1})	CuA (mol·L^{-1})
0 Cu	0.35	0.02	0.10	0.00
1.5 Cu				1.50
3.5 Cu				3.50

2.3. Sample characterization

For microstructural analysis, the samples were polished in an alumina suspension (0.25 μm) and immersed in an aqueous solution containing 10% nitric acid (HNO_3) and 5% hydrofluoric acid (HF) for approximately 5 s to reveal the microstructure. Microstructural and topographical analyses were performed using an optical microscope (Olympus Inc., model BX51M, USA). A scanning electron microscope (SEM; Carl Zeiss, model LS15 EVO, USA) was also used for imaging in secondary (SE) and backscattered (BSE) electron beam modes, with a voltage range of 15-20 kV. Structural analysis was carried out using X-ray diffraction (XRD) measurements with a Rigaku diffractometer, model MiniFlex 600, operating at 15 mA and 40 kV, in fixed time mode, with a Bragg-Brentano (θ-2θ) configuration, a step of 0.04°, a collection time of 1.6 seconds, and monochromatic Cu-Kα radiation (λ = 1.540456 Å). The HighScore Plus® software analyzed the diffracted peaks using crystallographic data sheets from the Crystallography Open Database (COD).

Semi-quantitative chemical microanalysis was conducted using energy-dispersive X-ray spectroscopy (EDS; Bruker, USA) in a detector coupled to the SEM equipment, operating at 15 kV, Fourier-transform infrared spectroscopy (FTIR; JASCO Corp, model FT/IR-410, USA) operating in absorbance mode at room temperature, with 120 scans and a resolution of 2 cm^{-1}, and Raman spectroscopy (Metrohm Raman spectrometer, model i-Raman Plus 532H, USA) operating with wavelength of 532 nm and laser power of 100%. Further chemical details were

acquired by X-ray photoelectron spectroscopy (XPS; Thermo Scientific, model Thermo K-alpha, USA) with an AlKα radiation source (1.486 eV) spot size of 400 μm, energy step of 200 eV for long scan (survey) and 50 eV for short scan spectra (high-resolution), with resolution of 1 eV for long and 0.01 eV for short scan, and energy correction using the C1s peak. The results were analyzed using CasaXPS® version 2.3.24 software.

Roughness values (Ra – average roughness and Rq – root mean square average roughness) were obtained by laser confocal microscopy (DCM3D, Leica, USA) with a resolution of 0.160 μm and a measurement range of 524 μm. The surface wettability was evaluated by measuring contact angles using a Ramé-Hart goniometer (Ramé-Hart Instrument Inc., Cedar Knolls, NJ, USA), model 100-00, with distilled water and diiodomethane (20 μL) drops at room temperature. Average values were obtained from three randomly selected droplets along the surface. Vickers microhardness values were obtained using a Shimadzu HMV-G instrument, with a load of 2.942 N and a dwell time of 15 seconds. Average values were calculated from 10 random measurements along the surface.

2.4. Biological evaluation

Cell viability and adhesion were analyzed using the MTT (3-(4,5-dimethylthiazol-2-yl)-2,5-diphenyltetrazolium bromide) and CV (crystal violet) colorimetric assays, where α-MEM (minimal essential medium) was conditioned with MC3T3-E1 (subclone 4; ATCC CRL-2593), a mouse pre-osteoblastic cell line. For the tests, 0.2 g/mL cells were cultured in α-MEM supplemented with 10% fetal bovine serum (FBS) at 37°C and 5% CO_2. Sub-confluent passages were trypsinized and used in all experiments. After 24 hours of incubation at 37°C, the conditioned medium was collected and tested for cell viability. A 5×10^4 cells/mL were seeded in 96-well plates, and after 24 hours at the sub-confluent stage, they were incubated for 24 hours and 72 hours with the conditioned medium (n = 6). Internal control was assayed by keeping the cells exposed to conventional culture medium (control).

After 24 hours and 72 hours, cell viability was evaluated using an MTT assay, and cell viability was estimated by measuring the absorbance in a microplate reader (SYNERGY-HTX multi-mode reader, Biotek, USA) at 570 nm wavelength. For the cell adhesion assay, pre-osteoblast cells were treated with conditioned medium for 24 hours. The cells were trypsinized, counted, and then reseeded at 5×10^4 cells/well in 96-well culture plates for 24 hours. Briefly, adherent cells were rinsed in warm phosphate-buffered saline (PBS) and then fixed in a 3:1 (v/v)

mixture of absolute ethanol and glacial acetic acid for 10 minutes at room temperature, followed by air-drying.

The adherent cells were stained with 0.1% crystal violet (w/v) for 10 min at room temperature. Excess dye was removed by decantation, and the sample was washed twice with distilled water. The dye was extracted with 10% acetic acid (v/v), and the optical density was measured at 540 nm using a microplate reader (Biotek Co., Winooski, VT). Data from each experiment were analyzed with six observations per group (n = 6).

3. RESULTS AND DISCUSSION

The current density *vs.* time plot of the MAO-treated samples is shown in **Fig. 1**. In the first seconds (**Fig. 1a**), there was a sharp decay in the current density in all samples, beginning around 2.0 – 3.0 A/cm^2 and achieving values below 0.5 A/cm^2. After that, the current densities remain at a plateau with minimal fluctuations over time. The zoomed view (**Fig. 1b**) indicates that the initial decay is not uniform for all samples, exhibiting a non-linear dependence on the amount of Cu in the electrolyte. As previously reported (Aliofkhazraei et al., 2021), the initial decay is due to rapid oxide growth induced by the anodic voltage, which acts as an insulator (dielectric) and prevents charge transfer from the electrolyte to the substrate. As charges accumulate in the coatings, dielectric breakdown eventually occurs, resulting in plasma discharges (micro-arcs) and gas bubble formation. Therefore, the noise in the plateau stage of the current density curves can be linked with the corresponding micro-arcs along the coating. This finding is consistent with some similar studies in the literature (Cardoso et al., 2023b; Tang et al., 2024), which found that increasing the Cu concentration in the electrode led to faster dielectric breakdown. This aligns with the present result, as the first dielectric drop occurred in the electrode with the highest copper concentration.

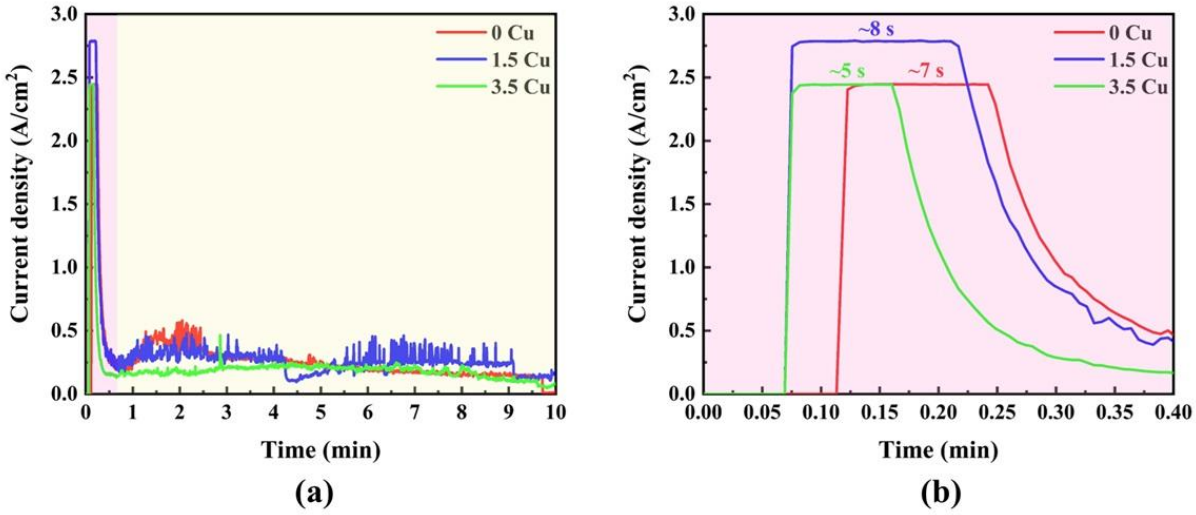

Fig. 1: Current density as a function of time: overall (a) and zoomed view (b).

The microstructure of the substrate and the corresponding topography of the MAO-treated samples are shown in **Fig. 2**. Overall, the substrate depicted some bright granular microstructure related to a TaMoNb-rich BCC phase and some dark precipitates in the boundaries, related to TiZr-rich HCP phase, agreeing well with our previous studies (Torrento et al., 2022). All the MAO-treated samples exhibited a typical porous coating, with no evidence of cracking at the microscale. The average pore size remained approximately 2.0 μm without modification, regardless of the Cu concentration in the electrolyte, indicating that the plasma energy and distribution could remain unchanged. As observed by Yao *et al.* (Yao et al., 2014), no obvious differences in low-magnification morphology were observed between the Cu-doped and Cu-free coatings, indicating that Cu incorporation had no significant effect on the coating surface morphology.

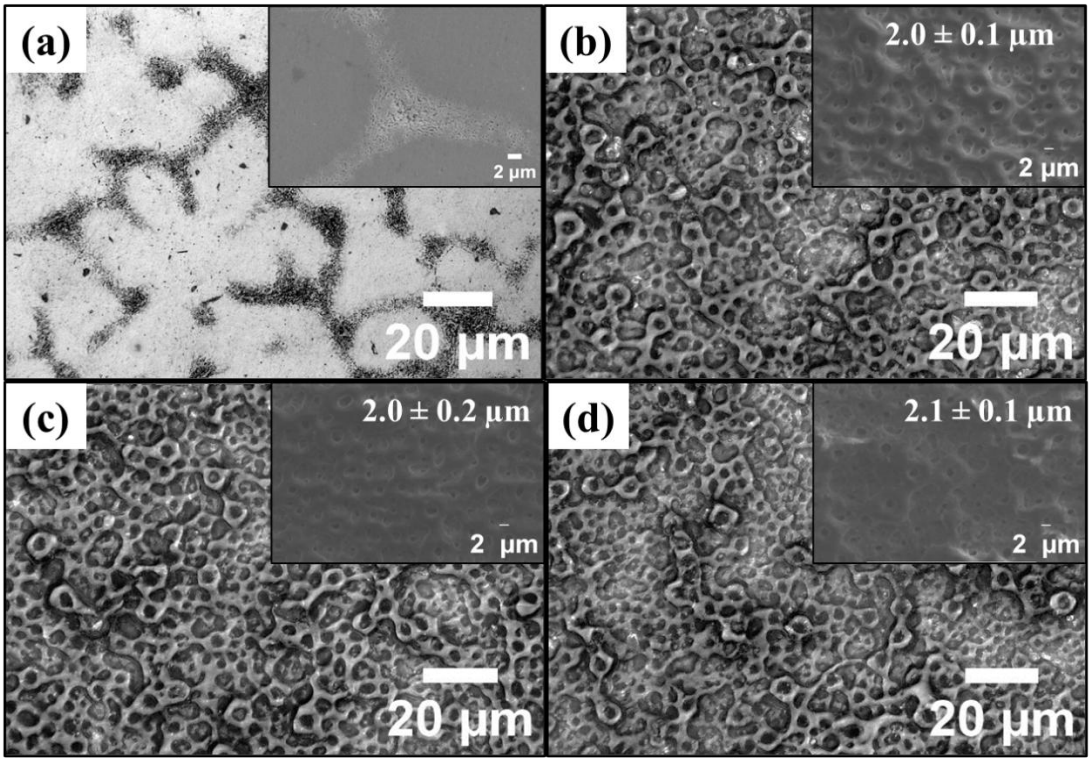

Fig. 2: Microstructure of the substrate (a), and topographical view of the MAO-treated samples: (b) 0 Cu, (c) 1.5 Cu, and (d) 3.5 Cu. SEM imaging and average pore size as an inset.

The phase proportions in the substrate and coatings are shown in **Fig. 3**. The substrate exhibits sharp peaks from the BCC phase (CIF #1523154), with some sparse peaks from the HCP phase (CIF #9008523) visible in the zoomed view, which agrees well with the phase proportions identified in **Fig. 2**. The MAO-treated samples depicted a pronounceable halo from amorphous phase below 40°, which could be probably formed during the dielectric breakdown and plasma discharges of the surface treatment. However, in the zoomed view, it is possible to identify some sparse peaks from the $CaCO_3$ (CIF #1010962), CaO (CIF #1011095), and $CaPO_4$ (CIF #1517238) phases, which could have formed during Ca- and P-enrichment in the outer layer. In addition to the overall XRD profiles remaining unchanged with the Cu concentration in the electrolyte, the BCC phase peaks were attenuated relative to the substrate, indicating the presence of a thick oxide layer on the surface. Similar results were detected by Sousa *et al.* (Sousa et al., 2024b), who found the same amorphous halo when applying MAO treatment to the TiZrNbTaMo HEA in a Cu-free electrolyte.

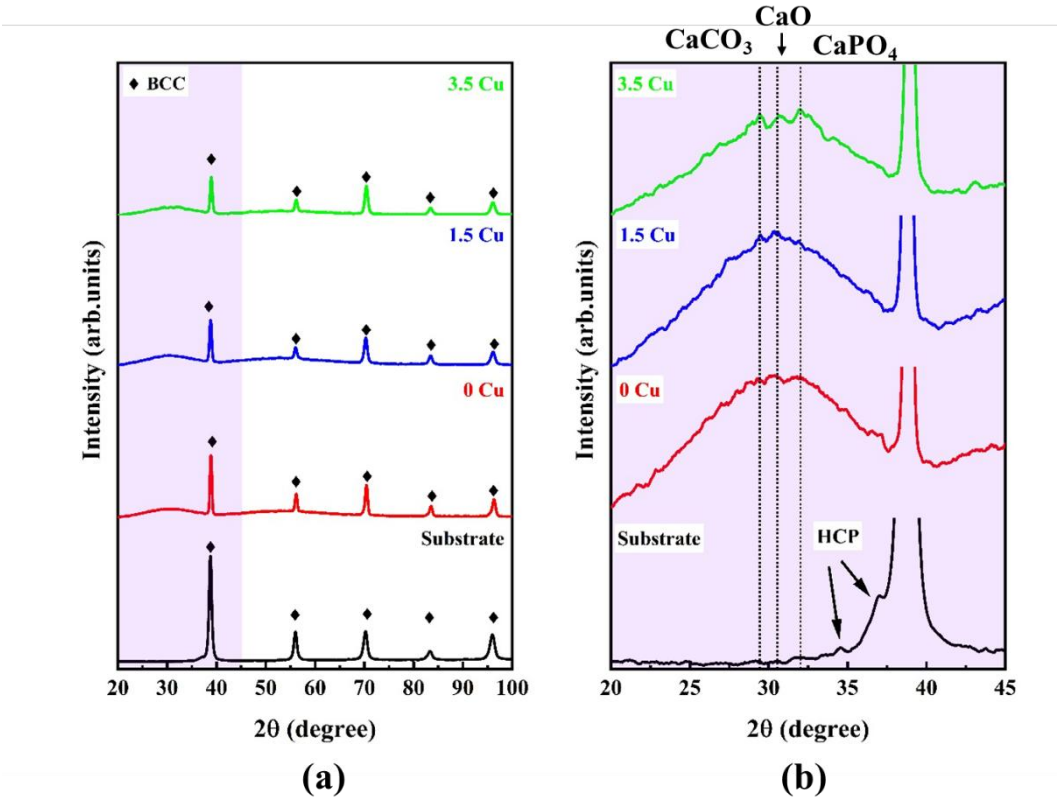

Fig. 3: XRD profile of the studied samples in an overall (a) and zoomed view (b).

The elemental EDS analysis of the samples is shown in **Fig. 4**. The substrate exhibits chemical segregation within the existing phases, with Ta enriched in the grains and Ti in the boundaries, which aligns with our previous studies (Torrento et al., 2022). Moreover, the MAO-treated samples exhibited a uniform distribution of the selected elements across the coatings, with no clear differences in Cu content. Chemical details are presented in the semi-quantitative EDS analysis, performed in the selected area mode and shown in **Fig. 5**. The overall chemical composition (**Fig. 5a**) indicates that the MAO-treated samples contain considerable amounts of O and C, likely in the form of oxides and carbonates, respectively. A look at the number of alloying elements (**Fig. 5b**) indicated that the proportion decreased significantly with the MAO treatment, with most of the Ti remaining, along with a secondary amount of Ta, Nb, and Zr, and Mo in trace amounts. This result indicates that, in addition to the multicomponent chemical composition of the substrate, the MAO coating is formed by distinct amounts of metallic elements, due to differences in the oxidative reactions of Ti and Ta, which are more reactive toward oxygen and tend to oxidize preferentially, forming stable oxides. In contrast, elements such as Mo, with lower oxygen affinity, are less prone to oxidation and therefore appear in smaller quantities within the oxide layer. Regarding the number of bioactive species (**Fig. 5c**), it is notable that although the

Mg concentration remained nearly constant, Ca and P exhibited fluctuations under each condition, suggesting a role for Cu in influencing electrolyte conductivity. The prevalence of Ca compared to Mg and P is directly related to its abundance in the electrolyte, resulting in a Ca/P ratio higher than that expected for the hydroxyapatite (1.67). Lastly, in **Fig. 5d**, the amount of incorporated Cu in the MAO coating can be compared. Interestingly, its chemical proportion decreased with increasing electrolyte concentration, supporting the assumption that Cu addition can improve electrical conductivity and favor dielectric breakdown and plasma discharges during MAO treatment. Moreover, the Cu concentration remained at a trace level in the MAO coatings (<0.1 at%), suggesting the potential to affect microorganisms without interfering with cells or tissues. As reported by Zong *et al.* (Zong et al., 2017), excessive Cu in nanotubes can be toxic to osteoblasts, but cytotoxicity can be ignored when the Cu content is relatively low, allowing integration of the favorable antibacterial activity of Cu with excellent biological properties.

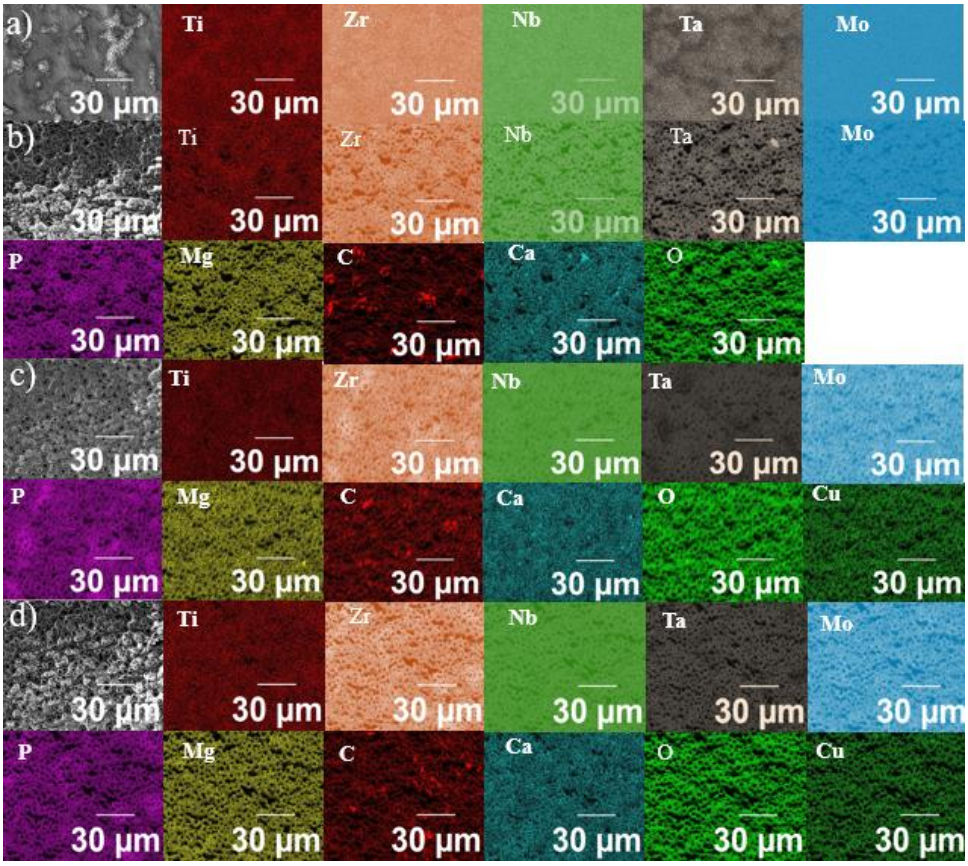

Fig. 4: Elemental EDS map of the samples: substrate (a), 0 Cu (b), 1.5 Cu (c), and 3.5 Cu (d).

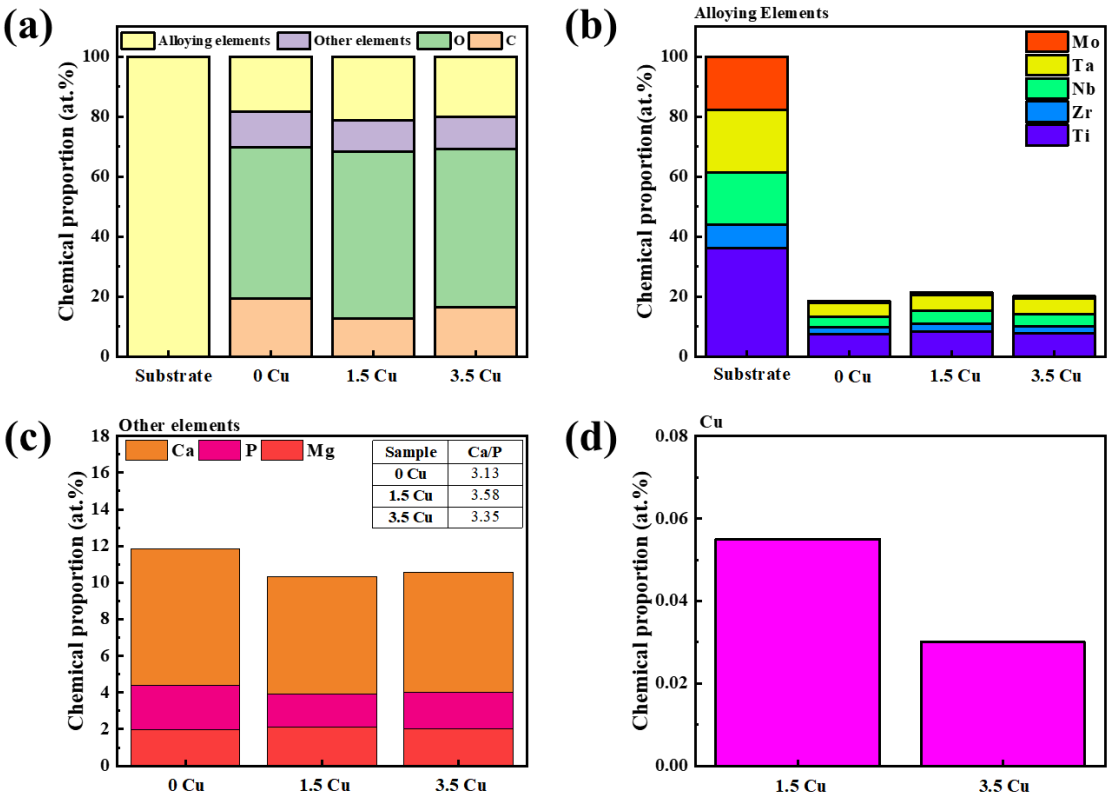

Fig. 5: Semi-quantitative EDS analysis of the samples: overall elements (a), alloying elements (b), bioactive elements (c), and Cu (d).

Spectroscopic FTIR and Raman analyses (**Fig. 6**) allowed identification of molecular radical groups in the coatings. Overall, the FTIR spectra of the MAO-treated samples were similar, with minor differences observed at low wavenumbers. The broad band observed around 3400 cm^{-1} is attributed to the O–H stretching vibration, indicating the presence of hydroxyl groups and/or adsorbed water molecules within the porous MAO surface. This hydrophilic character is typically associated with improved surface bioactivity and cell adhesion. The weak band near 1650 cm^{-1} corresponds to the H–O–H bending vibration of molecularly adsorbed water, which is consistent with the hydrophilic nature of the coatings. The absorption peak detected around 1450 cm^{-1} is assigned to the asymmetric stretching mode of carbonate ions (CO_3^{2-}). The intense band centered between 1050–1000 cm^{-1} corresponds to the asymmetric stretching vibration of phosphate groups (PO_4^{3-}), confirming the incorporation of phosphorus-containing species from the β-glycerophosphate electrolyte. These peaks were also identified in studies involving MAO coatings that incorporate calcium and phosphorus (Alipal et al., 2023; Coan et al., 2025). In the Raman spectrum, P-O bands were identified, corresponding to the bands reported by Stammeier

et al. (Stammeier et al., 2018). Additionally, Ti-O, Ca-O, C=C, and C-O bands were also identified and corroborated with the literature (Coan et al., 2025; Liu et al., 2016), supporting the results obtained by FTIR.

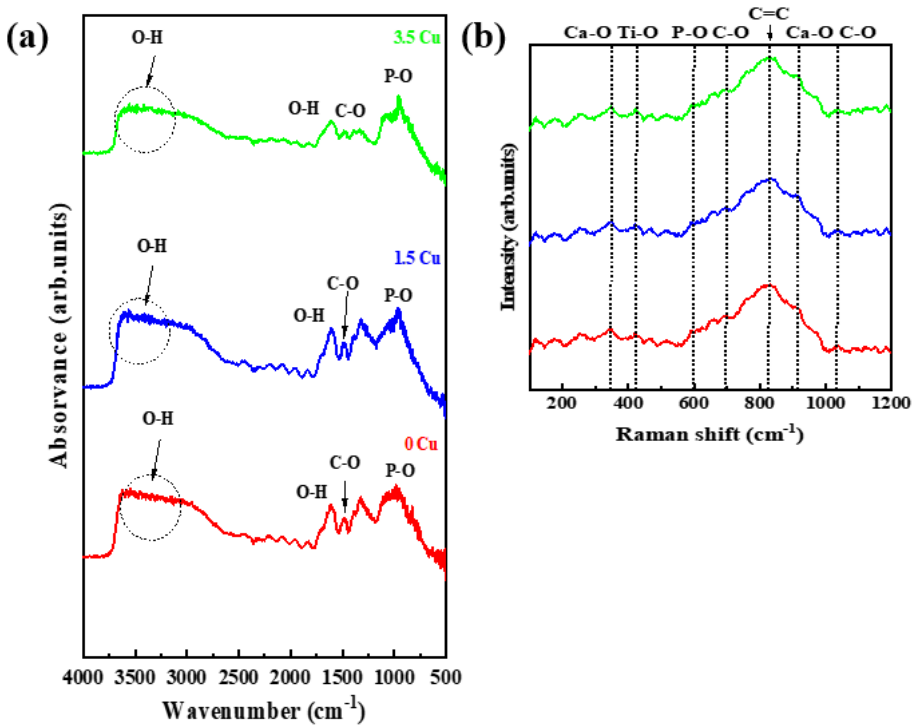

Fig. 6: Vibrational chemical analysis: FTIR spectra a), Raman spectra b)

XPS analysis (**Fig. 7**) was performed on MAO-treated samples containing Cu in the electrolyte to provide further details on the chemical composition of the outer layer. The survey spectra and the corresponding semi-quantitative analysis indicated the abundance of C and O in the outer layer, probably related to the formation of oxides, organic, and inorganic compounds during the MAO treatment. Ca and P elements were enriched with the addition of Cu to the electrolyte, but the Ca/P ratio differed from that observed in the EDS results. Given that EDS analysis has a greater penetration depth, it can be inferred that calcium (Ca) and phosphorus (P) are non-uniformly distributed in the MAO coating. Another relevant factor is that in the 3.5 Cu sample, neither Cu nor Mg was detected by XPS, indicating that these elements are in deeper regions of the coating. High-resolution XPS spectra (**Supplementary material**) revealed the presence of inorganic compounds (phosphate, $CaCO_3$, and $MgCO_3$), which are similar to those previously identified by our group (Costa et al., 2021; Sousa et al., 2019) . The copper was found as Cu_2O, and the possible reaction for the formation of this compound from the electrolyte was

$2Cu(CH_3COO)_2 + H_2O \rightarrow Cu_2O + 4CH_3COOH$. Furthermore, the copper Cu_2O was deconvoluted into three main components (C-C, C-O, and O=C), confirming the presence of carbonates, phosphates, and oxides in the coatings. Even at low concentrations, it is also possible to notice the presence of some alloying elements from the bulk in the more stable oxide form (TiO_2, ZrO_2, Nb_2O_5, Ta_2O_5, and MoO_3), almost the same oxides found by Sousa *et al.* (Sousa et al., 2024).

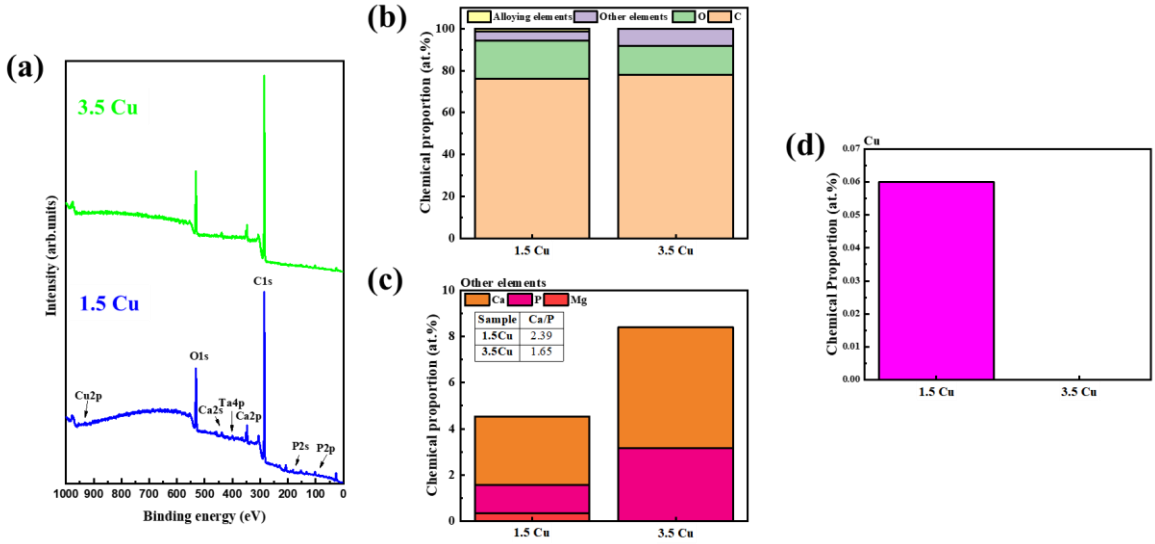

Fig. 7: XPS analysis of the Cu-rich MAO-treated samples: survey spectra (a), b) graphic of all elements, c) graphic of electrolyte elements, d) graphic of copper.

The samples (**Fig. 8a**) exhibited rougher surfaces than the substrate, due to micro-arc discharges and pore formation. The addition of Cu slightly reduced roughness, though further studies are needed to confirm this effect. Roughness remained in the micrometer range, which is beneficial for fixation in dental implants as studied by Wennerberg *et al.* (Wennerberg et al., 1995), who pointed out that implants with an average surface roughness of 0.9–1.3 µm and a homogeneous surface structure showed better fixation than implants with an average surface roughness of 0.4 µm and a clear surface pattern. The hardness was slightly higher than that of the substrate, due to the oxide layer, although the substrate's influence persisted despite the thin coating. Cu content did not significantly affect Vickers microhardness analysis (**Fig. 8b**). All samples in the contact angle measurements (**Fig. 8c**) exhibited hydrophilic behavior (contact angle < 90°) with a non-linear dependence on Cu content, suggesting that Cu influences electrolyte conductivity and oxidation processes. This behavior is relevant, as implants with

higher hydrophilicity are known to promote enhanced responses from osteogenic cells, facilitating early osseointegration and potentially increasing the overall success rate of implantation (Kazek-Kęsik et al., 2014; Zaniolo et al., 2022). However, certain characteristics of more hydrophobic surfaces may also confer advantages, as they tend to exhibit stronger bactericidal properties due to reduced bacterial adhesion (Jäger et al., 2017; Zaniolo et al., 2022). The polar component of the surface energy characterizes strong bonds between molecules (hydrogen, ionic, covalent, dipole-dipole bonds). In contrast, the dispersed component characterizes weak bonds of dispersion forces (van der Waals interactions). The results of surface energy analysis (**Fig. 8d**) showed that the surface energy was primarily dispersive, indicating the presence of organic compounds, which is consistent with the chemical analyses.

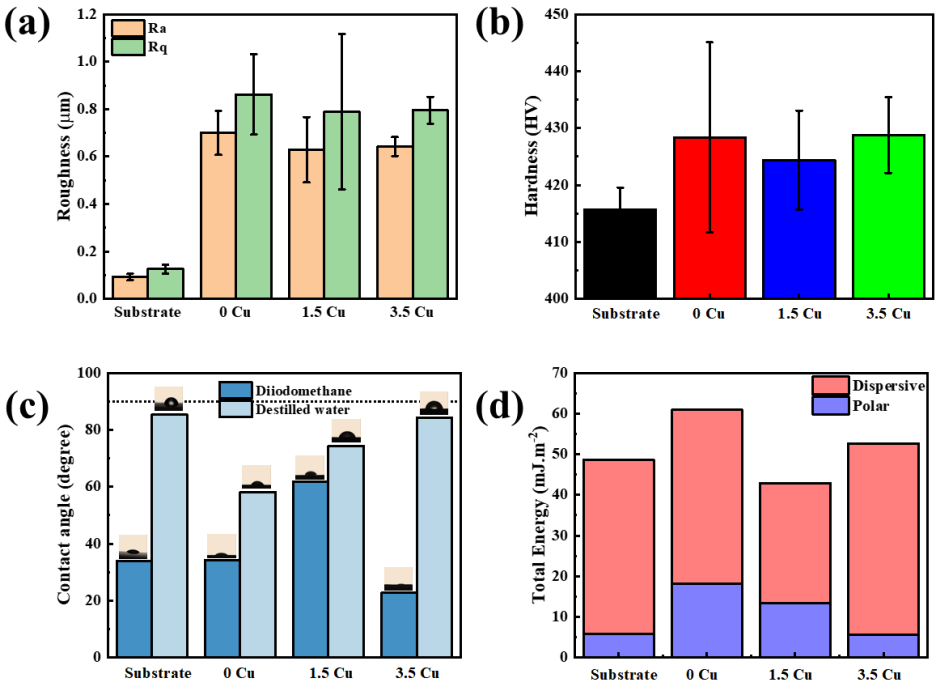

Fig. 8: Physicochemical characteristics of the surfaces: roughness (a), Vickers microhardness (b), contact angle (c), and surface energy (d).

The preliminary cytotoxicity analysis (**Fig. 9**) indicates that adding Cu to the electrolyte did not affect initial cell viability or adhesion. Overall, values were comparable to or higher than the control, indicating that the tested Cu levels were non-cytotoxic. Further studies may demonstrate the antimicrobial action of copper, as previous research has shown that even a low copper content can exhibit antibacterial properties, demonstrated by Shimabukuro *et al.*

(Shimabukuro et al., 2020), who showed that the copper-incorporated samples had no harmful effects on the proliferation and calcification of osteoblast-like cells. Moreover, inhibition of anaerobic bacterial growth was confirmed in these samples. The study also revealed that the antibacterial activity against *S. aureus* was prolonged and enhanced during immersion in physiological saline.

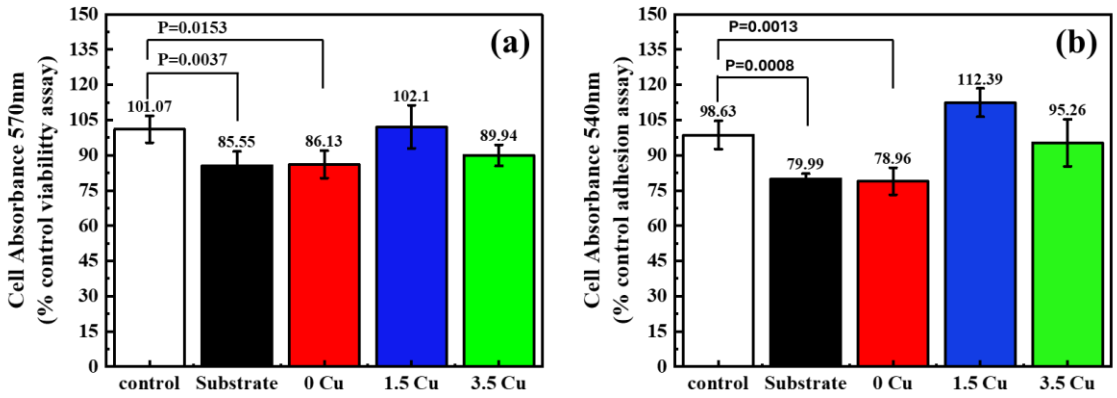

Fig. 9: In vitro cytotoxic results of the samples: MTT (a) and CV (b) assays.

4. Conclusion

In this study, the non-equiatomic TiZrNbTaMo HEA was micro-arc oxidized (MAO) in Cu-rich electrolytes to functionalize the surface for biomedical use. The Cu concentration modulated MAO processing, altering the timing of dielectric breakdown and plasma discharges. Untreated material showed a granular BCC matrix with small HCP precipitates at grain boundaries, whereas MAO-treated surfaces displayed the characteristic round-pore, porous topography. Consistent with this, the substrate's diffraction pattern featured a dominant BCC phase with shallow HCP peaks, while MAO-treated samples exhibited a pronounced amorphous halo with sparse reflections assigned to $CaCO_3$, CaO, and $CaPO_4$. The MAO process yielded homogeneous, crack-free porous oxide coatings with higher roughness than the substrate; all treated samples were hydrophilic, indicating improved wettability and the potential to enhance cell adhesion and proliferation. Compositional analyses (EDS, FTIR, Raman, XPS) confirmed incorporation of bioactive species (Ca, P, Mg) and minor Cu - mainly as Cu_2O - within an oxide layer comprising stable phases such as TiO_2, ZrO_2, Nb_2O_5, Ta_2O_5, and MoO_2. Preliminary 24 h in vitro assays showed that Cu addition did not induce cytotoxicity and maintained or improved cell

viability and adhesion relative to controls, suggesting that Cu-enriched coatings preserve biocompatibility while potentially conferring antibacterial functionality. Collectively, these findings advance bio-high-entropy alloys by demonstrating that MAO in Cu-rich media can simultaneously promote bioactivity, surface stability, and antibacterial potential, offering a promising pathway for multifunctional metallic biomaterials for long-term orthopedic and bone-fixation implants.

Funding

This study was funded by the National Council for Scientific and Technological Research (CNPq; grants #314.810/2021-8, #404020/2023–2, #421.677/2023-6, #408594/2024-1, #100704/2024-7, and #312391/2025-0) and São Paulo Research Foundation (FAPESP; grants #2021/13921–3, #2024/03886-4, #2024/14878-2, and #2024/03148–3) funding agencies.

Conflicts of interest

The authors declare that they have no known competing financial interests or personal relationships that could have influenced the work reported in this paper.

Availability of data and material

The data can be shared upon request.

Code availability

Not applicable.

Authors' contributions

Samuel Phelippe Bonetti: Writing – original draft, Visualization, Validation, Formal analysis, Data curation. **Tiago dos Santos Pereira de Sousa:** Writing – review & editing, Validation, Investigation, Formal analysis. **Jhuliene Elen Muro Torrento:** Writing – review & editing, Validation, Investigation, Formal analysis. **Gerson Santos de Almeida:** Data curation,

Validation. **William Fernando Zambuzzi:** Data curation, Validation. **Carlos Roberto Grandini:** Writing – review & editing, Validation, Resources. **Diego Rafael Nespeque Correa:** Writing – review & editing, Supervision, Resources, Project administration, Methodology, Funding acquisition, Conceptualization.

Acknowledgment

The authors thank Professor F.M.L. Pontes and Professor L.G. Possato from the Department of Chemistry (UNESP - Campus Bauru) for the XRD and Raman measurements, Professor P.N. Lisboa-Filho from the Department of Physics and Meteorology (UNESP – Campus Bauru) for the confocal imaging, and Professor E.C. Rangel from the Laboratory of Technological Plasmas (UNESP – Campus Sorocaba) for the wettability measurements. The authors are also grateful to the Brazilian Nanotechnology National Laboratory (LNNano) at the Brazilian Center for Research in Energy and Materials (CNPEM) for the XPS experiments (Proposal #20241166).

5. References

1. W.-L. Hsu, C.-W. Tsai, A.-C. Yeh, and J.-W. Yeh: Clarifying the four core effects of high-entropy materials. *Nat Rev Chem* 8(6), 471 (2024).
2. L. Li, Z. Liu, X. An, and W. Sun: Design methods of high-entropy alloys: Current status and prospects. *J Alloys Compd* 1029, 180638 (2025).
3. J. Adhikari, P. Saha, P. Mandal, S. K. Sinha, A. H. Seikh, J. A. Mohammed, and M. Ghosh: A Review on High Entropy Alloys as Metallic Biomaterials: Fabrication, Properties, Applications, Challenges, and Future Prospects. *Biomedical Materials & Devices* (2025).
4. M. Todai, T. Nagase, T. Hori, A. Matsugaki, A. Sekita, and T. Nakano: Novel TiNbTaZrMo high-entropy alloys for metallic biomaterials. *Scr Mater* 129, 65 (2017).
5. N. Hua, W. Wang, Q. Wang, Y. Ye, S. Lin, L. Zhang, Q. Guo, J. Brechtl, and P. K. Liaw: Mechanical, corrosion, and wear properties of biomedical Ti–Zr–Nb–Ta–Mo high entropy alloys. *J Alloys Compd* 861 (2021).
6. S. P. Wang and J. Xu: TiZrNbTaMo high-entropy alloy designed for orthopedic implants: As-cast microstructure and mechanical properties. *Materials Science and Engineering: C* 73, 80 (2017).
7. G. Li, F. Ma, P. Liu, S. Qi, W. Li, K. Zhang, and X. Chen: Review of micro-arc oxidation of titanium alloys: Mechanism, properties and applications. *J Alloys Compd* 948, 169773 (2023).

8. X. Ming, Y. Wu, Z. Zhang, and Y. Li: Micro-Arc Oxidation in Titanium and Its Alloys: Development and Potential of Implants. *Coatings* 13(12), 2064 (2023).
9. X. He, X. Zhang, X. Wang, and L. Qin: Review of Antibacterial Activity of Titanium-Based Implants' Surfaces Fabricated by Micro-Arc Oxidation. *Coatings* 7(3), 45 (2017).
10. G. C. Cardoso, K. Barbaro, P. A. B. Kuroda, A. De Bonis, R. Teghil, I. I. Krasnyuk, L. Imperatori, C. R. Grandini, and J. V. Rau: Antimicrobial Cu-Doped TiO2 Coatings on the β Ti-30Nb-5Mo Alloy by Micro-Arc Oxidation. *Materials* 17(1), 156 (2023).
11. T. S. P. Sousa, J. E. M. Torrento, P. A. B. Kuroda, V. R. M. Gonçalves, K. S. Coan, D. R. N. Correa, and C. R. Grandini: Surface aspects of novel Bio-HEAs MAO-treated in a Ca-, P-, and Mg-rich electrolyte. *Appl Surf Sci* 664, 160227 (2024).
12. M. Aliofkhazraei, D. D. Macdonald, E. Matykina, E. V. Parfenov, V. S. Egorkin, J. A. Curran, S. C. Troughton, S. L. Sinebryukhov, S. V. Gnedenkov, T. Lampke, F. Simchen, and H. F. Nabavi: Review of plasma electrolytic oxidation of titanium substrates: Mechanism, properties, applications and limitations. *Applied Surface Science Advances* 5(May), 100121 (2021).
13. J. Tang, F. Wei, L. Zhao, L. Yang, J. Li, Z. Sun, C. Yang, W. Zhang, and B. Liu: Superior antibacterial properties of copper-doped titanium oxide films prepared by micro-arc oxidation. *Ceram Int* 50(1), 1370 (2024).
14. J. E. Torrento, T. D. S. P. De Sousa, N. Cristino Da Cruz, G. Santos De Almeida, W. F. Zambuzzi, C. R. Grandini, and D. R. Nespeque Correa: Development of non-equiatomic Bio-HEAs based on TiZrNbTa-(Mo and Mn). *APL Mater* 10(8) (2022).
15. X. Yao, X. Zhang, H. Wu, L. Tian, Y. Ma, and B. Tang: Microstructure and antibacterial properties of Cu-doped TiO2 coating on titanium by micro-arc oxidation. *Appl Surf Sci* 292, 944 (2014).
16. M. Zong, L. Bai, Y. Liu, X. Wang, X. Zhang, X. Huang, R. Hang, and B. Tang: Antibacterial ability and angiogenic activity of Cu-Ti-O nanotube arrays. *Materials Science and Engineering: C* 71, 93 (2017).
17. K. S. Coan, T. dos S. Pereira de Sousa, C. R. Grandini, E. C. Rangel, N. C. da Cruz, K. Barbaro, M. Fosca, J. V. Rau, S. A. Tsipas, and D. R. Nespeque Correa: Addressing wear-resistant, bioactive, and bio-selective coatings on the biomedical Ti-6Al-4 V alloy by performing MAO treatment in TMO-rich electrolyte. *Appl Surf Sci* 689, 162557 (2025).
18. J. Alipal, S. Saidin, A. Z. K. Lo, P. Koshy, H. Z. Abdullah, M. I. Idris, and T. C. Lee: In vitro surface efficacy of CaP-based anodised titanium for bone implants. *Surfaces and Interfaces* 39, 102872 (2023).

19. J. A. Stammeier, B. Purgstaller, D. Hippler, V. Mavromatis, and M. Dietzel: In-situ Raman spectroscopy of amorphous calcium phosphate to crystalline hydroxyapatite transformation. *MethodsX* 5, 1241 (2018).
20. J. Liu, R. Caracas, D. Fan, E. Bobocioiu, D. Zhang, and W. L. Mao: High-pressure compressibility and vibrational properties of (Ca,Mn)CO3. *American Mineralogist* 101(12) (2016).
21. T. S. P. Sousa, N. D. A. Da Costa, D. R. N. Correa, L. A. Rocha, and C. R. Grandini: Morphology, crystalline structure and chemical composition of MAO treated Ti-15Zr-Mo surfaces enriched with bioactive ions. *Materials Research* 22(6) (2019).
22. N. A. Costa, D. R. N. Correa, P. N. Lisboa-Filho, T. S. P. Sousa, C. R. Grandini, and L. A. Rocha: Influence of the molybdenum on characteristics of oxide films produced by micro-arc oxidation on Ti-15Zr-based alloys. *Surf Coat Technol* 408(December 2020), 126856 (2021).
23. A. Wennerberg, T. Albrektsson, B. Andersson, and J. J. Krol: A histomorghometric study of screw-shaped and removal torque titanium implants with three different surface topographies. *Clin Oral Implants Res* 6(1), 24 (1995).
24. A. Kazek-Kęsik, M. Krok-Borkowicz, E. Pamuła, and W. Simka: Electrochemical and biological characterization of coatings formed on Ti–15Mo alloy by plasma electrolytic oxidation. *Materials Science and Engineering: C* 43, 172 (2014).
25. K. M. Zaniolo, S. R. Biaggio, J. A. Cirelli, M. A. Cominotte, N. Bocchi, and R. C. Rocha-Filho: Physical characterization and biological tests of bioactive titanium surfaces prepared by short-time micro-arc oxidation in green electrolyte. *Mater Res Express* 9(2), 025401 (2022).
26. M. Jäger, H. P. Jennissen, F. Dittrich, A. Fischer, and H. L. Köhling: *Materials* 10, (2017).
27. M. Shimabukuro, Y. Tsutsumi, K. Nozaki, P. Chen, R. Yamada, M. Ashida, H. Doi, A. Nagai, and T. Hanawa: Investigation of antibacterial effect of copper introduced titanium surface by electrochemical treatment against facultative anaerobic bacteria. *Dent Mater J* 39(4), 639 (2020).

Supplementary Material

Supplementary material

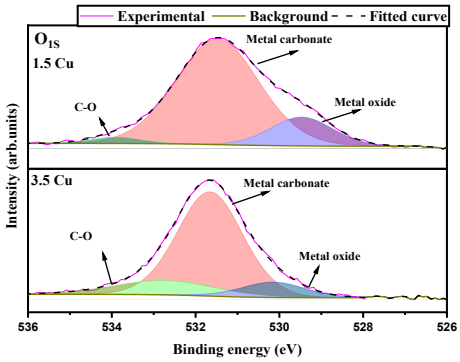

O1s

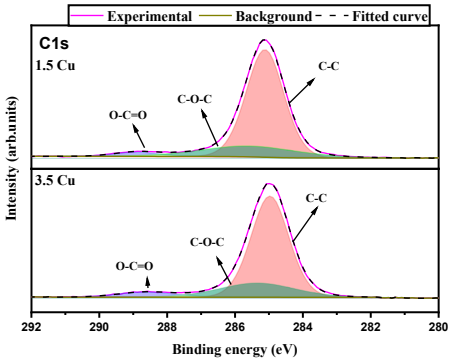

C1s

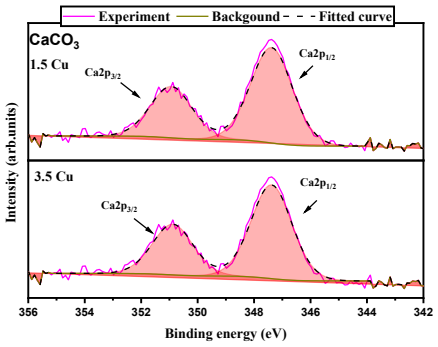

Ca2p

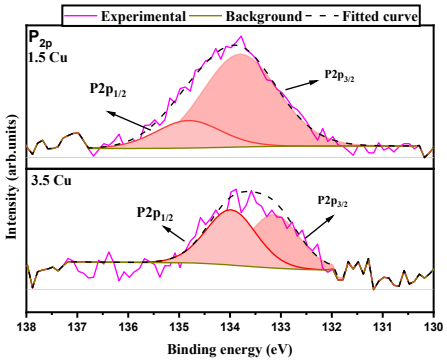

P2p

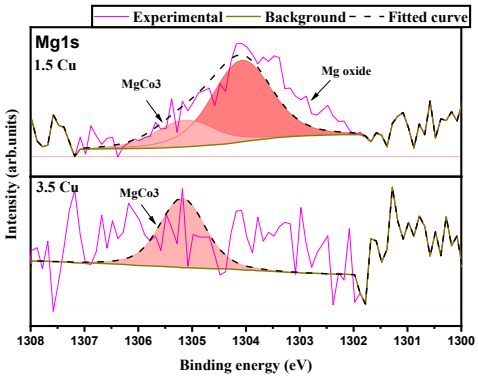

Mg1s

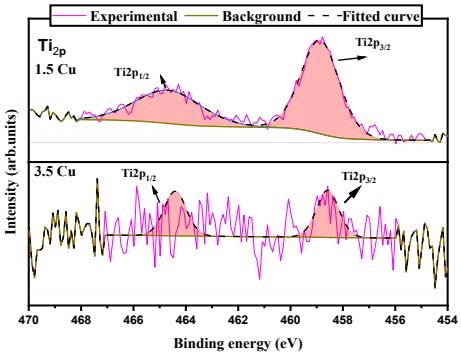

Ti2p

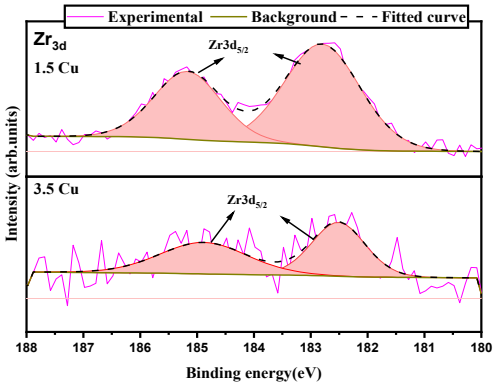

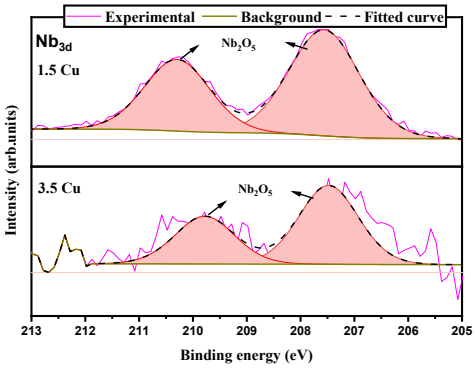

Nb3d

Zr3d

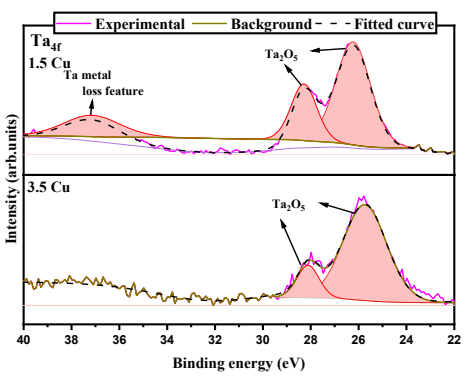

Ta4f

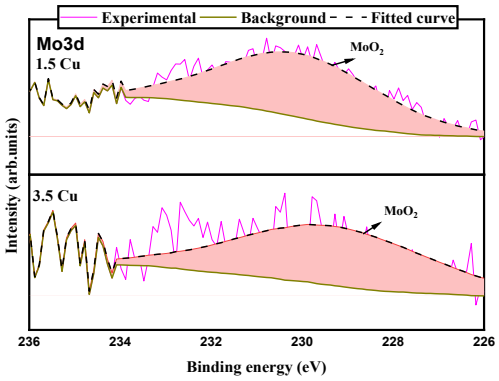

Mo3d

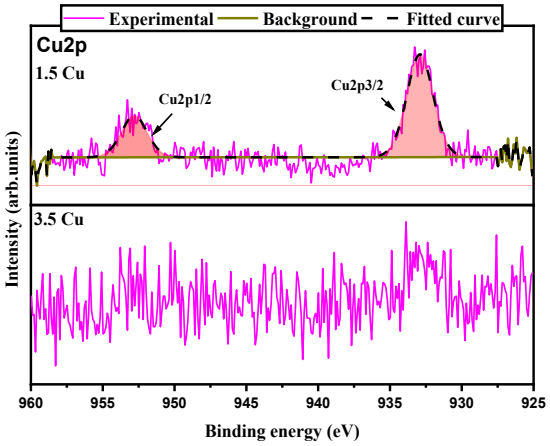

Cu2p

Fig. S1: HR spectrum of studied elements.

Table S1: Quantitative results of the HR XPS analysis.

Sample	*Spectrum*	*Residual*	*Chemical designation*	*Proportion (%)*	*Peak position (eV)*
1.5 Cu	*O1s*	*1.13*	*Metal carbonate*	*80.81*	*531.68*
			C-O	*2.82*	*534.18*
			Metal oxide	*16.73*	*530.08*
	Ti2p	*0.90*	TiO_2	*100.00*	*458.88 ($p_{3/2}$)* *464.78 ($p_{1/2}$)*
	Zr3d	*0.95*	ZrO_2	*100.00*	*182.70*
	Nb3d	*1.15*	Nb_2O_5	*100.00*	*207.18*
	Ta4f	*1.14*	Ta_2O_5	*80.80*	*26.28*
			Ta metal loss feature	*19.20*	*37.18*
	Mo3d	*1.07*	MoO_3	*100.00*	*229.68*
	C1s	*1.07*	*C-C*	*77.00*	*288.98*
			C-O	*19.52*	*286.18*
			O=C-O	*3.49*	*285.08*
	Ca2p	*0.91*	$CaCO_3$	*100.00*	*347.28 ($p_{3/2}$)* *350.88 ($p_{1/2}$)*
	P2p	*1.11*	PO_4^{3-}	*100.00*	*133.78 ($p_{3/2}$)* *134.88 ($p_{1/2}$)*
	Mg1s	*0.84*	$MgCO_3$	*24.78*	*1305.28*
			MgO	*75.22*	*1304.08*
	Cu2p	*1.09*	Cu_2O	*100.00*	*932.88($p_{3/2}$)* *952.68($p_{1/2}$)*
3.5 Cu	*O1s*	*0.87*	*Metalcarbonate*	*74.02*	*531.68*
			C-O	*10.41*	*533.28*
			Metal oxide	*15.57*	*530.08*
	Ti2p	*1.12*	TiO_2	*100.00*	*458.63 ($p_{3/2}$)* *464.34 ($p_{1/2}$)*
	Zr3d	*1.15*	ZrO_2	*100.00*	*182.48*
	Nb3d	*1.04*	Nb_2O_5	*100.00*	*207.48*
	Ta4f	*1.07*	Ta_2O_5	*100.00*	*25.78*
	Mo3d	*1.05*	MoO_3	*100.00*	*229.98*
	C1s	*1.11*	*C-C*	*73.92*	*288.88*
			C-O	*20.42*	*285.68*
			O=C-O	*5.69*	*288.58*
	Ca2p	*1.02*	$CaCO_3$	*100.00*	*347.30 ($p_{3/2}$)* *350.88 ($p_{1/2}$)*
	P2p	*0.94*	PO_4^{3-}	*100.00*	*133.31 ($p_{3/2}$)* *134.02 ($p_{1/2}$)*
	Mg1s	*0.88*	$MgCO_3$	*100.00*	*1305.28*

4 Considerações finais

Diante dos resultados obtidos, pode-se concluir que o presente trabalho demonstrou o potencial da HEA TiZrNbTaMo funcionalizada por oxidação por MAO como um material promissor para aplicações biomédicas. O processo de MAO possibilitou a formação de

revestimentos estáveis, homogêneos e porosos, com incorporação eficaz de íons bioativos e variação controlada de cobre no eletrólito, o que influenciou positivamente as propriedades químicas, físico-químicas e biológicas da superfície.

As análises mostraram que o aumento da concentração de cobre promoveu maior hidrofilicidade e rugosidade superficial, condições que favorecem a adesão e proliferação celular, sem causar efeitos citotóxicos nos testes preliminares. Além disso, a presença de elementos como cálcio, fósforo e magnésio reforçou o caráter bioativo do revestimento, contribuindo para uma melhor integração com o tecido ósseo.

Dessa forma, o estudo evidencia que a técnica de MAO aplicada a HEAs representa uma abordagem eficiente para o desenvolvimento de superfícies multifuncionais voltadas à área da saúde.

Por fim, ressalta-se que este trabalho abre caminho para novas pesquisas, incluindo estudos de longo prazo sobre o comportamento antimicrobiano, a resistência mecânica e de desgaste dos revestimentos e testes *in vivo*, que poderão consolidar ainda mais o uso dessas ligas como biomateriais de próxima geração.

5 Referências

ABDEL-HADY GEPREEL, Mohamed; NIINOMI, Mitsuo. Biocompatibility of Ti-alloys for long-term implantation. Journal of the Mechanical Behavior of Biomedical Materials, v. 20, p. 407–415, 1 abr. 2013.

CARDOSO, Giovana Collombaro et al. *Antimicrobial Cu-Doped TiO2 Coatings on the β Ti-30Nb-5Mo Alloy by Micro-Arc Oxidation. Materials, v. 17, n. 1, p. 156, 27 dez. 2023.*

CASTRO, Diogo et al. *An Overview of High-Entropy Alloys as Biomaterials. Metals, v. 11, n. 4, p. 648, 15 abr. 2021.*

DAVIS, Rahul et al. *A comprehensive review on metallic implant biomaterials and their subtractive manufacturing. International Journal of Advanced Manufacturing TechnologySpringer Science and Business Media Deutschland GmbH, , 1 maio 2022.*

GAO, Yu et al. *High-entropy oxides for catalysis: Status and perspectives. Applied Catalysis A: General, v. 631, p. 118478, 5 fev. 2022.*

HE, Xiaojing et al. *Antibacterial ability and osteogenic activity of porous Sr/Ag-containing TiO 2 coatings. Biomedical Materials, v. 11, n. 4, p. 045008, 10 ago. 2016.*

HSU, Wei-Lin et al. *Clarifying the four core effects of high-entropy materials. Nature Reviews Chemistry, v. 8, n. 6, p. 471–485, 2024.*

J BIJLSMA, J. W. et al. *Arthritis 1 Osteoarthritis: an update with relevance for clinical practiceLancet.* [S.l.: S.n.]. *Disponível em: <www.thelancet.com>.*

KARAFLOU, Maria; GOULIS, Dimitrios G. The growing challenge of aging populations: Addressing health and societal impacts. Maturitas, v. 202, p. 108720, 1 nov. 2025.

KIM, Jeoung Han et al. *Mechanical properties and deformation twinning behavior of as-cast CoCrFeMnNi high-entropy alloy at low and high temperatures. Materials Science and Engineering: A, v. 712, p. 108–113, 17 jan. 2018.*

LV, Linhe et al. *Recent advances in high-entropy alloys for biomedical applications. Materials and DesignElsevier Ltd, , 1 out. 2025.*

MA, Ning et al. *Research Progress of Titanium-Based High Entropy Alloy: Methods, Properties, and Applications. Frontiers in Bioengineering and Biotechnology, v. 8, 11 nov. 2020.*

MAHMUD, Md Zobair Al et al. *Emerging breakthroughs in biomaterials for orthopedic applications: A comprehensive review. Bioprinting, v. 36, p. e00323, 1 dez. 2023.*

MARADIT KREMERS, Hilal et al. *Prevalence of Total Hip and Knee Replacement in the United States. The Journal of Bone and Joint Surgery-American Volume, v. 97, n. 17, p. 1386–1397, set. 2015.*

MING, Xinwei et al. *Micro-Arc Oxidation in Titanium and Its Alloys: Development and Potential of Implants. Coatings, v. 13, n. 12, p. 2064, 9 dez. 2023.*

MIRACLE, D. B.; SENKOV, O. N. A critical review of high entropy alloys and related concepts. Acta MaterialiaElsevier Ltd, , 1 jan. 2017.

NG, Chun et al. *Entropy-driven phase stability and slow diffusion kinetics in an Al 0.5CoCrCuFeNi high entropy alloy. Intermetallics, v. 31, p. 165–172, dez. 2012.*

ROTELLA, Giovanna et al. *Surface Functionalization of Metallic Biomaterials: Present Trend and Future Perspectives.* In*:* [S.l.: S.n.]*. p. 295–341.*

SOUSA, T. S. P. et al. *Surface aspects of novel Bio-HEAs MAO-treated in a Ca-, P-, and Mg-rich electrolyte. Applied Surface Science, v. 664, p. 160227, ago. 2024.*

THANIGAIVEL, S. et al. *Insight on recent development in metallic biomaterials: Strategies involving synthesis, types and surface modification for advanced therapeutic and biomedical applications. Biochemical Engineering Journal, v. 187, p. 108522, 1 nov. 2022.*

THARANI KUMAR, S. et al. *Review of Metallic Biomaterials in Dental Applications. Journal of pharmacy & bioallied sciences, v. 12, n. Suppl 1, p. S14–S19, ago. 2020.*

WEN, Xueying et al. *Micro-arc oxidation (MAO) and its potential for improving the performance of titanium implants in biomedical applications. Frontiers in Bioengineering and Biotechnology, v. 11, 7 nov. 2023.*

XU, Yuqing et al. *In-situ high throughput synthesis of high-entropy alloys. Scripta Materialia, v. 160, p. 44–47, 1 fev. 2019.*

YU, Bingxi et al. *Recent progress in high-entropy alloys: A focused review of preparation processes and properties. Journal of Materials Research and Technology, v. 29, p. 2689–2719, 1 mar. 2024.*

ZHANG, Ge et al. *Dual-structured oxide coatings with enhanced wear and corrosion resistance prepared by plasma electrolytic oxidation on Ti-Nb-Ta-Zr-Hf high-entropy alloy. Surface and Coatings Technology, v. 456, p. 129254, mar. 2023.*

ZHANG, Xiangyu et al. *Effects of copper nanoparticles in porous TiO2 coatings on bacterial resistance and cytocompatibility of osteoblasts and endothelial cells. Materials Science and Engineering: C, v. 82, p. 110–120, jan. 2018.*

6 Documentos comprobatórios

6.1 Submissão de artigo

[Materials] Manuscript ID: materials-4004192 - Submission Received

Editorial Office <materials@mdpi.com>
para Diego, mim, Jhuliene, Carlos, Tiago, Gerson, William

Dear Professor Correa,

Thank you very much for uploading the following manuscript to the MDPI submission system. One of our editors will be in touch with you soon.

Journal name: Materials
Manuscript ID: materials-4004192
Type of manuscript: Article
Title: Surface engineering of non-equiatomic TiZrNbTaMo HEA by MAO treatment in a Cu-rich electrolyte for biomedical applications
Authors: Samuel P. Bonetti, Jhuliene E. M. Torrento, Carlos R. Grandini, Tiago dos S. P. de Sousa, Gerson S. de Almeida, William F. Zambuzzi, Diego R. N. Correa *
Received: 7 Nov 2025
E-mails: samuel.bonetti@unesp.br, jhuliene.torrento@unesp.br, carlos.r.grandini@unesp.br, tiago.sousa@unesp.br, gs.almeida@unesp.br, w.zambuzzi@unesp.br, diego.correa@unesp.br
Metals and Alloys
https://www.mdpi.com/journal/materials/sections/metals_alloys
New Advances in High Entropy Alloys
https://www.mdpi.com/journal/materials/special_issues/E4WA3X7T7M

6.2 Autorização dos coautores para utilização de artigo em um TCC

AUTORIZAÇÃO DOS COAUTORES PARA UTILIZAÇÃO DE ARTIGO COMO TRABALHO DE CONCLUSÃO DE CURSO

Eu, Samuel Phelippe Bonetti, aluno do curso de Bacharelado de Física de Materiais da Faculdade de Ciências da UNESP de Bauru, venho por meio deste documento, solicitar autorização para a utilizar o artigo intitulado “Surface engineering of non-equiatomic TiZrNbTaMo HEA by MAO treatment in a Cu-rich electrolyte for biomedical applications”, do qual sou autor, como base para meu trabalho de conclusão de curso (TCC)

-Titulo: Surface engineering of non-equiatomic TiZrNbTaMo HEA by MAO treatment in a Cu-rich electrolyte for biomedical applications

-Autores: Samuel Phelippe Bonetti, Jhuliene Elen Muro Torrento, Carlos Roberto Grandini, Tiago dos Santos Pereira de Sousa, Gerson Santos de Almeida, William Fernando Zambuzzi, Diego Rafael Nespeque Correa.

Declaro que o uso do artigo respeitará os créditos devidos a todos os coautores, mantendo a integridade do conteúdo original e assegurando que qualquer modificação necessária será previamente alinhada com os envolvidos se aplicável.

Solicito, portanto, a anuência formal dos coautores mediante a assinatura abaixo, para que o artigo seja utilizado como parte do meu TCC, conforme as diretrizes acadêmicas da faculdade de ciências da UNESP, campus de Bauru

Documento assinado digitalmente
JHULIENE ELEN MURO TORRENTO
Data: 17/11/2025 14:25:18-0300
Verifique em https://validar.iti.gov.br

MSc.Jhuliene Elen Muro Torrento

Documento assinado digitalmente
CARLOS ROBERTO GRANDINI
Data: 17/11/2025 17:56:07-0300
Verifique em https://validar.iti.gov.br

Prof. Dr. Carlos Roberto Grandini

Documento assinado digitalmente
TIAGO DOS SANTOS PEREIRA DE SOUSA
Data: 17/11/2025 18:19:37-0300
Verifique em https://validar.iti.gov.br

Dr. Tiago dos Santos Pereira de Sousa

Documento assinado digitalmente
GERSON SANTOS DE ALMEIDA
Data: 18/11/2025 10:19:25-0300
Verifique em https://validar.iti.gov.br

Dr. Gerson Santos de Almeida

Documento assinado digitalmente
WILLIAN FERNANDO ZAMBUZZI
Data: 04/12/2025 09:10:14-0300
Verifique em https://validar.iti.gov.br

Prof. Dr. William Fernando Zambuzzi

Documento assinado digitalmente
DIEGO RAFAEL NESPEQUE CORREA
Data: 17/11/2025 14:17:12-0300
Verifique em https://validar.iti.gov.br

Prof. Dr. Diego Rafael Nespeque Correa

Documento assinado digitalmente
SAMUEL PHELIPPE BONETTI
Data: 17/11/2025 13:32:06-0300
Verifique em https://validar.iti.gov.br

Samuel Phelippe Bonetti

Bauru- SP, 17 de novembro de 2025